SLAC-PUB-653

DETERMINATION OF THE TOTAL PHOTON-PROTON CROSS SECTION FROM HIGH ENERGY INELASTIC ELECTRON SCATTERING

E. D. Bloom, R. L. Cottrell, D. H. Coward, H. DeStaebler, Jr.,
J. Drees, G. Miller, L. W. Mo, R. E. Taylor
Stanford Linear Accelerator Center
Stanford University, Stanford, California 94305

J. I. Friedman, G. C. Hartmann, and H. W. Kendall
Department of Physics and Laboratory for Nuclear Science
Massachusetts Institute of Technology, Cambridge, Massachusetts 02139

ERRATUM

Reference 11 is actually two references. The reference corresponding to the total γ-p cross sections measurements, (page 8, paragraph three, Figure 2) is:

Aachen-Berlin-Bonn-Hamburg-Heidelberg-München collaboration, Phys. Letters 27B, 54 (1968).

The reference corresponding to the πN^* cross section measurements, (page 8, paragraph a) is the given reference 11.

(This paper will also be submitted to Phys. Rev. Letters)

SLAC-PUB-653
September 1969
(TH) and (EXP)

DETERMINATION OF THE TOTAL PHOTON-PROTON CROSS SECTION FROM HIGH ENERGY INELASTIC ELECTRON SCATTERING*

E. D. Bloom, R. L. Cottrell, D. H. Coward, H. DeStaebler, Jr.,
J. Drees,** G. Miller, L. W. Mo, R. E. Taylor
Stanford Linear Accelerator Center
Stanford University, Stanford, California 94305

J. I. Friedman, G. C. Hartmann,† and H. W. Kendall
Department of Physics and Laboratory for Nuclear Science††
Massachusetts Institute of Technology, Cambridge, Massachusetts 02139

ABSTRACT

The total photoabsorption cross section of hydrogen can be obtained from inelastic electron proton scattering cross sections by extrapolating to the limit of zero four-momentum transfer. Using the Stanford Linear Accelerator 20-GeV spectrometer facility, the absolute cross section for the reaction $e + p \rightarrow e + x$, where x is any final state, has been measured from hydrogen at a laboratory scattering angle of 1.5°. The incident electron energy varied between 5 and 20 GeV. Only the final state electron was detected. After radiative corrections, the scattering data are used to extract $\sigma_{\gamma p}$ for energies from pion threshold to an equivalent real photon energy of about 15 GeV. The range of q^2 covered by the data extends from 0.013 to 0.26 $(GeV/c)^2$.

(Submitted to the International Symposium on Electron and Photon Interactions at High Energies, Daresbury, September, 1969)

---

*Work supported in part by the U.S. Atomic Energy Commission.

**On leave from Bonn University, Bonn, Germany.

†Now at Xerox Corporation, Rochester, New York.

††Work supported in part through funds provided by the Atomic Energy Commission under contract No. AT(30-1)2098.

In the limit of zero four-momentum transfer, inelastic electron scattering can be directly related to the total photoproduction cross section. We have measured inelastic electron-proton scattering cross sections at 1.5^{o} laboratory angle for incident electron energies between 5 and 20 GeV. By extrapolating from these cross sections to zero four-momentum transfer, we obtain values for the total photoproduction cross section from the proton, $\sigma_{\gamma p}$, from pion threshold to 15 GeV/c incident photon momentum.

Hand has shown that in the one photon approximation the inelastic cross section can be written[1]:

$$\frac{d^2\sigma}{d\Omega dE'} = \Gamma_t(E,E',\theta)\left[\sigma_T(W,q^2) + \epsilon(E,E',\theta)\,\sigma_S(W,q^2)\right]$$

where the virtual photon spectrum of the electron is given by

$$\Gamma_t(E,E',\theta) = \frac{\alpha}{4\pi^2}\,\frac{K}{q^2}\,\frac{E'}{E}\,\frac{2}{1-\epsilon}$$

and the polarization parameter

$$\epsilon(E,E',\theta) = \frac{1}{1 + 2\left(1+\nu^2/q^2\right)\tan^2\theta/2}$$

ϵ is near unity for all the measurements in this experiment.

In these equations:

E = initial electron energy in lab. system

E' = scattered electron energy in lab. system

θ = laboratory scattering angle

$q^2 = 4\,EE'\sin^2\theta/2$ = (four momentum transfer)^2

$\nu = E - E'$ = energy transfer

$W = \left(M^2 + 2M\nu - q^2\right)^{1/2}$ = invariant mass of the final hadronic state

$K = \frac{W^2 - M^2}{2M}$ = real photon energy required to produce a state of of mass W

M = mass of the proton

$\sigma_T(W, q^2)$ and $\sigma_S(W, q^2)$ are the total cross sections for transverse and longitudinal polarization of a virtual photon. As $q^2 \longrightarrow 0$ gauge invariance implies

$$\sigma_T(W, q^2) \longrightarrow \sigma_{\gamma p}(W)$$

$$\sigma_L(W, q^2) \longrightarrow 0 \ (q^2)$$

By extrapolating values of $(d^2\sigma/d\Omega dE')/\Gamma_t$, we obtain values of $\sigma_{\gamma p}(W)$.

The choice of kinematics for obtaining $d^2\sigma/d\Omega dE'$ is governed by several factors. At very forward angles, electromagnetic processes dominate the cross sections, and electron-electron scattering from the orbital electrons in the hydrogen target gives large backgrounds. On the other hand, the smaller the angle, the more reliable are the extrapolations. We require measurements at several initial energies for a given angle to facilitate model independent radiative corrections. We chose to measure cross sections at $\theta = 1.5^\circ$ for the following 9 values of the incident energy E = 5.0, 7.1, 9.3, 11.8, 13.8, 15.6, 17.3, 18.1, and 20.0 GeV. For each initial energy, measurements were made for many secondary energies to obtain cross sections at values of W which were closely spaced through the resonance region, $W \leq 2$ GeV. Above $W \approx 2$ GeV cross sections were obtained at intervals of 0.25 GeV in W for values of E' above 4 GeV.

The SLAC 20 GeV/c spectrometer facility was used for the measurements. The electron beam entered the experimental area after momentum analysis. Various values of $\Delta p/p$ between .1% and 1% were used. The direction of the beam was controlled by observing the position of the beam on retractable fluorescent screens separated by about 70 feet. The estimated uncertainty in the beam

direction was ± .1 mrad which results in a 1.5% uncertainty in the cross section for 1.5^{o}. To cover the wide range of beam currents (10^{8} - 10^{12} electrons/sec) used in the experiment, three kinds of beam monitors were used: two toroidal (induction) monitors for high currents; a thin walled H_2 ion chamber for low currents and a secondary emission quantameter (SEQ) whose range overlapped both the toroids and the ion chamber. The SEQ was also used as the beam stop. From cross checks among the monitors and frequent calibrations using a Faraday cup, the estimate of probable systematic error in monitoring the number of incident electrons was ± 1%.

The primary electrons were scattered in a 7-cm long condensed liquid hydrogen target. After scattering, particles were momentum analyzed in the SLAC 20-GeV spectrometer.[2] This spectrometer focussed particles onto a system of four hodoscopes so that a reconstruction of the final trajectory was possible. The momentum resolution of the system was $\Delta p/p = .1\%$, and the angular resolution was $\Delta\theta = .3$ mr.

Electrons were identified by observing the pulse height in a lead-lucite total absorption shower (T.A.) counter. A fast logic trigger consisting of an "or" between two scintillation counters in coincidence and the T.A. counter gated the hodoscope information, T.A. pulse height, and the other information into a set of buffers. These buffers were then read into an SDS 9300 on-line computer which wrote the information from each event on magnetic tape and also performed a preliminary on-line analysis.

An off-line analysis was performed to obtain the measured cross sections.[3] These cross sections have errors arising from counting statistics and random systematic errors (from beam monitors, angular errors, etc.) of 2% added in quadrature. In addition, an overall systematic error of ± 3% is estimated.

Before the data are used for extrapolation to $q^2 = 0$, corrections must be applied for radiative processes. At small scattering angles, the radiative "tail" of the elastic peak contributes a significant fraction of the total rate. The fractional contribution of the elastic tail increases markedly with decreasing q^2 and increasing W, e.g.:

at $\theta = 1.5^o$, W = 4.4, $q^2 = 0.1$ the tail contributes 40%;

at $\theta = 1.5^o$, W = 4.4, $q^2 = 0.035$ the tail increases to 70%.

The radiative tail of the elastic peak includes contributions from internal bremsstrahlung and from radiative straggling in the target walls, liquid hydrogen and vacuum windows. The tail due to internal bremsstrahlung can be calculated to lowest order in α (single photon emission)[4] using the known form factors of the proton. The contribution due to straggling can be calculated, including the effects of multiple photon emission.[4] Since multiple photon emission also contributes to the tail of the internal processes, we have made a correction for this effect. In the straggling calculation factors of the form $(\ell n(E/E'))^t/\Gamma(1+t)$ are applied to the single photon formulae to take account of multiple photon emission. We have applied the same factors to the single photon approximation for internal bremsstrahlung. In order to obtain values of t for this purpose, we have constructed a peaking approximation which agreed within 1% with the exact calculation to lowest order in α. From this peaking approximation we extracted values of $t(E, E', \theta)$, the number of equivalent radiation lengths.

The inclusion of multiple photon effects is most important near π-threshold and for low E' where the tail is a major fraction of the cross section. At π-threshold, where the total measured yield is due to the elastic tail, our calculation agrees with the measured cross section. Multiple photon effects at the end of the measured spectra were largest for E = 20 GeV, E' = 4 GeV where their inclusion

changes the cross section due to the elastic tail by 6%, compared to a calculation neglecting multiple photons. We assign an error of ± 4% to the tail calculation everywhere.

After subtraction of the elastic tail from each measured spectrum, the data were corrected for radiative effects in the continuous part of the spectrum. All measured data were processed by a two-dimensional unfolding procedure based on the peaking approximation.[3,4] Errors were propagated through the unfolding program. To check the uncertainty of the numerical calculation, we used different interpolation and extrapolation techniques resulting in differences of typically .1 standard deviation and nowhere more than .8 standard deviation in the final cross section. The errors due to approximations in the theoretical formula are more difficult to estimate. However, studies indicate that at the small scattering angle of 1.5^{o}, these should add no more than ± 2% to the error of the final cross section.

The next step in the reduction of the data to $\sigma_{\gamma p}(W)$ is the extrapolation of $(d^2\sigma/d\Omega dE')/\Gamma_t$, (see Eq. (1)), to $q^2 = 0$. $d^2\sigma/d\Omega E'$ is the radiatively corrected experimental cross section. The resulting $\sigma_{\gamma p}(W)$ depends to some extent on the form of the extrapolation function. Present theory is not adequate to specify an extrapolation function, not even near the N*(1238) resonance, which has been investigated extensively, so we have used various simple functions.

The situation at four different values of W is illustrated in Fig. 1 in which each indicated data point arises from one measured spectrum, and as W increases, fewer spectra contribute. Near the first resonance (Fig. 1a), the decrease at small q^2 may arise from threshold angular momentum effects[5] or from the threshold dependence of $\sigma_L(W, q^2)$. A similar decrease is not seen elsewhere, for example, near the second resonance, shown in Fig. 1b. Figure 1c is typical for W between 2.2 and 3.6 GeV where at least seven spectra contribute to the q^2 plot;

here the errors on $\sigma_{\gamma p}$, arising from a fit to the data points, may be as small as 4%. Figure 1d is representative for higher W where fewer spectra contribute to the q^2 plot, and where the errors for $\sigma_{\gamma p}$ increase.

The final fits used for W < 2.3 GeV were the lowest order polynomials in q^2 that would give good fits in a χ^2 sense to the measured data. In the neighborhood of the first resonance we used parabolic fits with the three parameters redetermined at each value of W (for example, see the solid curve in Fig. 1a). Beyond the first resonance and for W < 2.3 GeV we used straight line fits with the two parameters redetermined at each value of W (for example, see the solid curve in Fig. 1b). For W > 2.3 GeV the slopes of the separate straight line fits at each W were consistent with a single value. A least squares fit to all slopes was made resulting in an average slope of $(-1.30 \pm .13)\ (\mathrm{GeV/c})^{-2}$. The final fits in this W range were $a(W)\ (1 - 1.30\ q^2)$, with a(W) refitted at each value of W (for example, see the solid curves in Figs. 1c and 1d). To check the dependence of the extrapolation procedure on the q^2 form used, several fits were made for W > 2.3 GeV.

Example 1: $\left(\frac{d^2\sigma}{d\Omega dE'}\right)/\Gamma_t = (a + b/\sqrt{K})\ f(q^2)$ for various $f(q^2)$

was fitted to all inelastic cross sections with W > 2.3 GeV. Three forms of $f(q^2)$ were tried, $f(q^2) = 1 + a\,q^2$, $f(q^2) = 1 + a\,q^2 + b\,q^4$, and $f(q^2) = \frac{1}{1 + a\,q^2}$. All of these fits gave results which deviated at most by 2% from their mean, for all W > 2.3 GeV This gives confidence that the form actually used for the extrapolation, $1 + a(W)\ q^2$, adequately describes the observed q^2 dependence.

Example 2: a vector dominance model[6] was fitted for each W. This model agreed with the final result to 2.5% on the average and nowhere deviated by more than .8 of a standard deviation.

The cross section obtained for $\sigma_{\gamma p}(W)$ is shown in Fig. 2. The error bars indicated are derived from the error matrix of the fit used in the extrapolation. In addition, we estimate possible systematic errors of ± 8% for W < 2 GeV. The dashed curves for W > 2 GeV indicate an estimate of systematic error in this region. These estimates were obtained by increasing all measured cross sections by 2%, decreasing the elastic tail by 3% and then carrying through new radiative corrections for the continuous part of the spectrum and another extrapolation to obtain the top curve. Similarly, by decreasing measured cross sections by 2% and increasing the elastic tail by 3%, etc., the bottom curve was obtained. Table 1 gives the values of $\sigma_{\gamma p}$ displayed in Fig. 2. Part (a) contains $\sigma_{\gamma p}$ and the errors resulting from our fits for $W \leq 2.01$, part (b) contains $\sigma_{\gamma p}$ for $W \geq 2.26$ and the estimates of systematic errors.

We have checked the overall normalization of our cross sections by comparing the elastic e-p cross sections obtained for each incoming energy with previously reported results[7] at similar values of q^2. We found agreement to within 3%.

Figure 2 includes some previous published values of $\sigma_{\gamma p}(W)$.[8,9,10,11] The dotted line shows the fit of Ref. 8 to the region of the N*(1238). The agreement is excellent. The other results shown are bubble chamber measurements. The agreement with the results from Refs. 9 and 10 is satisfactory, but there is a significant discrepancy with results from Ref. 11.

Some interesting features of the data are:

a. An apparent shoulder on the N*(1512) resonance at a mass $W \approx 1430$. This shoulder can be qualitively understood using the results of Ref. 11 on πN^* production, which has a rapid threshold dependence in this mass region. A phase shift analysis with more data than just the total cross section is needed to determine whether or not this shoulder is a manifestation of a resonance in this mass region.

b. The excitation of the N*(1512) relative to the other observed resonances appears to be a factor of 2 to 3 times greater than the corresponding excitation in $(\sigma_{\pi^- p} + \sigma_{\pi^+ p})/2$.[12] In general, the resonances appear quite strongly excited in photoproduction.

c. As mentioned earlier, we have fitted the inelastic e-p scattering data with an expression of the form[13]: $(A + B/\sqrt{K})\ (1 + a\ q^2)$ for $K \geq 3$ GeV. The result of this fit for $q^2 = 0$ is:

$$\sigma_{\gamma p}(K) = (108 + 68/\sqrt{K})\ \mu b$$

which implies a cross section at $K = \infty$ of $108 \pm 7\ \mu b$. The slope of the fit is $d\sigma_{\gamma p}/d(1/\sqrt{K}) = 68 \pm 17$. The errors quoted are obtained from the fitting procedure and no attempt has been made to include the estimated systematic errors. The errors quoted are also highly correlated. The error matrix of the fit implies $\Delta\sigma_{\gamma p} = \sqrt{49 + 289/K - 207/\sqrt{K}}$.

We wish to acknowledge the assistance of Dr. C. Jordan during the data taking for the experiment. We express our gratitude to all those who operated the accelerator during the runs, the H_2 target group and the Research Area department for their help in setting up the experiment. The critical alignment of beams and the spectrometer was carried out by the alignment group under W. Milner. Finally, we acknowledge the work of the spectrometer group under Mr. E. Taylor and thank Mr. M. Breidenbach for his work on the counter systems.

REFERENCES

1. See L. Hand, Proceedings of the 1967 Symposium on Electron and Photon Interactions at High Energies, or F. J. Gilman, Phys. Rev. 167, 1365 (1968).
2. Brief descriptions of the spectrometer and the hodoscopes may be found in W.K.H. Panofsky, Vol. I, Proceedings of the International Symposium on Electron and Photon Interactions at High Energies, Hamburg, Germany, (1965), (Springer-Verlag, Berlin, 1965); and A. M. Boyarski, F. Bulos, W. Busza, R. Diebold, S. D. Ecklund, G. E. Fischer, J. R. Rees, and B. Richter, Phys. Rev. Letters 20, 300 (1968).
3. E. Bloom et al., Report No. SLAC-PUB-642, Stanford Linear Accelerator Center, Stanford University, Stanford, California (1968) (to be published).
4. L. W. Mo, and Y. S. Tsai, Rev. Mod. Phys. 41, 205 (1969).
5. J. D. Bjorken and J. D. Walecka, Annals of Physics 38, 35 (1966).
6. J. J. Sakurai, Phys. Rev. Letters 22, 1078 (1969). $\xi(K)$ was assumed to be 1.
7. T. Janssens, R. Hofstader, E. B. Hughes, and M. R. Yearian, Phys. Rev. 142, 922 (1966). Comparison was made to the best fit reported Eq. 6, p. 930.
8. J. T. Beale, S. D. Ecklund, and R. L. Walker, Report No. CTSL-42, California Institute of Technology (1966).
9. SLAC-Tufts-UCB/LRL Collaboration, Report No. SLAC-PUB-618 (1969) (to be published).
10. J. Ballam, G. B. Chadwick, Z.G.T. Guiragossián, P. Klein, A. Levy, M. Menke, E. Pickup, P. Seyboth, T. H. Tan, and G. Wolf, Phys. Rev. Letters 21, 1544 (1968).
11. Aachen-Berlin-Bonn-Hamburg-Heidelberg-München Collaboration, Phys. Rev. 175, 1669 (1968).

12. See for instance G. Höhler, G. Ebel, and J. Giesecke, Z. Physik 180, 430 (1964) and A. A. Carter, K. F. Riley, R. J. Tapper, D. V. Bugg, R. S. Gilmore, K. M. Knight, D. C. Salter, G. H. Stafford, E.J.N. Wilson, J. D. Davies, J. D. Dowell, P. M. Hattersley, R. J. Homer, and A. W. O'Dell, Phys. Rev. 168, 1457 (1968).

13. An energy dependence of this type is suggested by total cross section measurements for purely hadronic processes, e.g., $\pi^+ p$, $\pi^- p$, $K^- p$, etc.

14. H. L. Lynch, J. V. Allaby, and D. M. Ritson, Phys. Rev. 164, 1635 (1967).

TABLE CAPTIONS

1a. $\sigma_{\gamma p}$ is the total photoabsorption cross section on hydrogen, in units of 10^{-30} cm^2, inferred from inelastic e-p scattering cross sections for $\theta = 1.5^{o}$. The errors arise from the random errors on the cross sections propagated through the extrapolation procedure as described in the text. Systematic errors, estimated to be ± 8%, are not shown in the table. W and K are in GeV.

1b. $\sigma_{\gamma p}$ is given for W > 2. σ_L and σ_H (in 10^{-30} cm^2) illustrate the effect of estimated systematic errors on the cross section as described in the text.

FIGURE CAPTIONS

1. Double differential cross section divided by Γ_t vs. q^2 at (a) W = 1.23 GeV, (b) W = 1.50 GeV, (c) W = 2.51 GeV, (d) W = 4.20 GeV. The solid curves indicate the fits used for the extrapolation of $\sigma_{\gamma p}$ to $q^2 = 0$. The extrapolated values, including the errors calculated from the error matrix of the fit, are shown as black points at $q^2 = 0$. The results of previous measurements[14] are also included.

2. The total γp absorption cross section, $\sigma_{\gamma p}$, as a function of W (or K). The data points are the extrapolated values, and the errors are calculated from the error matrix of the extrapolation procedure. The two dashed lines for W ≥ 2.26 GeV indicate the effect of our estimate of possible systematic errors, as described in the text. These lines correspond to σ_L and σ_H in Table 1b.

TABLE 1a

W	K	$\sigma_{\gamma p}$
1.110	.188	78.8 ± 41
1.125	.205	118.9 ± 38
1.140	.223	168.2 ± 34
1.155	.242	202.4 ± 31
1.170	.260	323.4 ± 32
1.185	.279	387.1 ± 34
1.120	.298	504.2 ± 37
1.215	.318	532.6 ± 37
1.230	.337	542.3 ± 32
1.245	.357	480.8 ± 30
1.260	.377	411.0 ± 31
1.275	.397	311.9 ± 33
1.290	.418	249.6 ± 31
1.305	.438	210.9 ± 26
1.320	.459	174.2 ± 27
1.335	.481	188.8 ± 26
1.350	.502	176.4 ± 25
1.365	.524	167.1 ± 17
1.380	.546	191.2 ± 17
1.395	.568	218.5 ± 17
1.410	.590	209.1 ± 18
1.425	.613	233.5 ± 16
1.440	.636	238.5 ± 16
1.455	.659	245.6 ± 18
1.470	.682	251.4 ± 18
1.485	.706	273.9 ± 19
1.500	.730	289.1 ± 20
1.515	.754	286.6 ± 19
1.530	.778	275.1 ± 18
1.545	.803	258.7 ± 16
1.560	.828	231.6 ± 17

Table 1a (cont.)

W	K	$\sigma_{\gamma p}$
1.575	.853	229.9 ± 17
1.590	.878	226.6 ± 16
1.605	.904	199.8 ± 17
1.620	.929	233.6 ± 18
1.635	.956	211.7 ± 16
1.650	.982	221.0 ± 15
1.665	1.008	232.4 ± 15
1.680	1.035	223.4 ± 16
1.695	1.062	241.6 ± 17
1.710	1.089	232.4 ± 18
1.725	1.117	223.8 ± 16
1.740	1.144	207.9 ± 15
1.755	1.172	159.3 ± 17
1.770	1.200	184.1 ± 18
1.785	1.229	175.3 ± 15
1.800	1.258	152.6 ± 15
1.815	1.286	155.6 ± 16
1.830	1.316	180.6 ± 16
1.845	1.345	159.9 ± 16
1.860	1.375	164.3 ± 17
1.875	1.404	116.0 ± 17
1.890	1.435	196.8 ± 16
1.905	1.465	170.8 ± 14
1.920	1.495	158.1 ± 14
1.935	1.526	175.4 ± 16
1.950	1.557	165.0 ± 16
1.965	1.589	163.7 ± 15
1.980	1.620	164.0 ± 15
1.995	1.652	141.7 ± 14
2.010	1.684	142.3 ± 14

TABLE 1b

W	K	σ_L	σ_H	$\sigma_{\gamma p}$
2.26	2.253	137	156	146.3 ± 8
2.510	2.888	136	158	148.2 ± 5
2.760	3.590	131	150	141.7 ± 5
3.010	4.359	129	145	136.8 ± 5
3.260	5.195	128	142	134.2 ± 5
3.510	6.097	127	142	133.2 ± 5
3.760	7.065	128	144	134.0 ± 6
4.01	8.100	120	136	125.2 ± 6
4.26	9.202	125	143	133.6 ± 8
4.510	10.371	120	139	130.4 ± 7
4.76	11.606	116	138	128.3 ± 9
5.01	12.907	107	132	119.3 ± 12
5.26	14.276	100	139	112.1 ± 18
5.50	15.7	108	172	139.9 ± 25

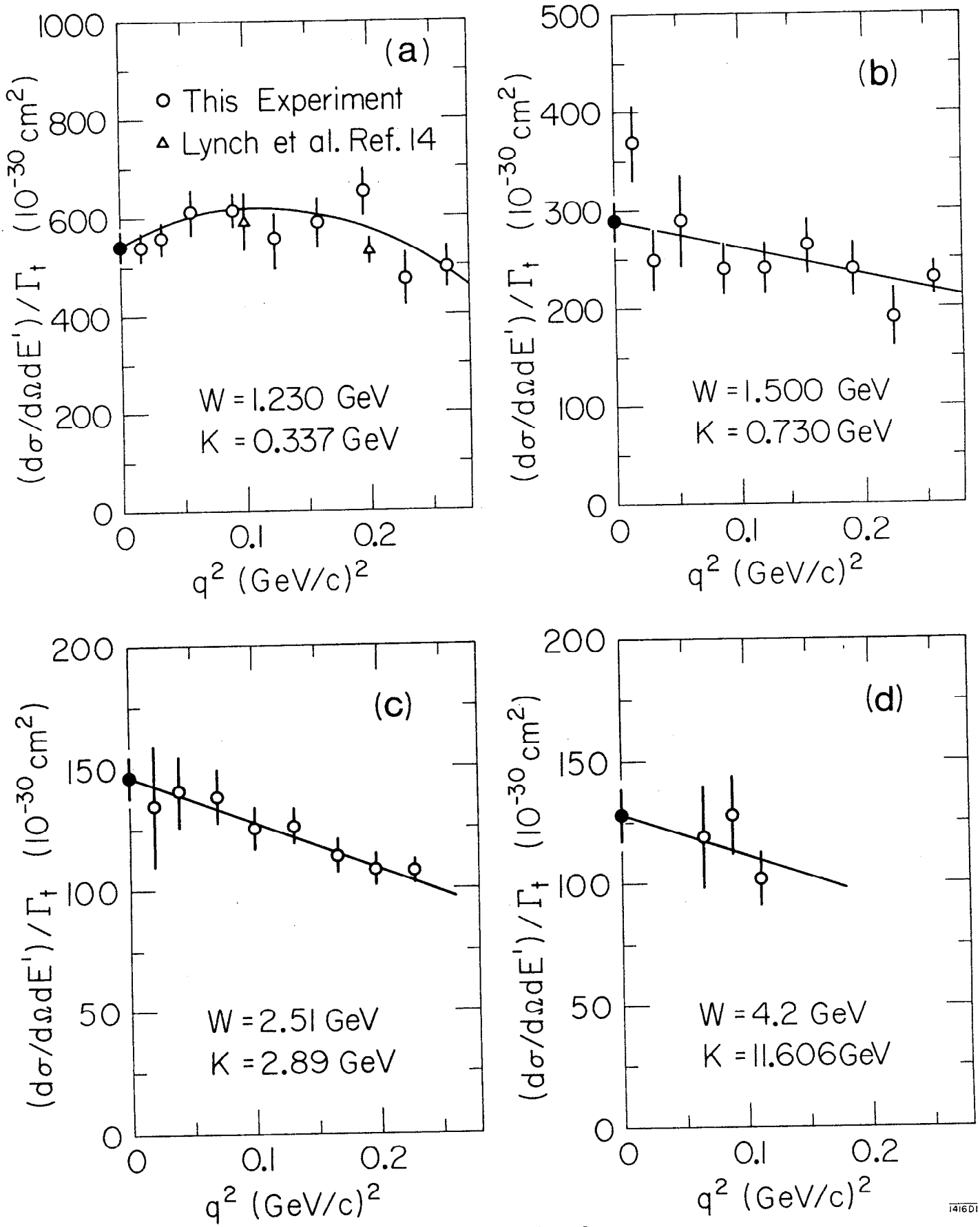
(a)
This Experiment
Lynch et al. Ref. 14
W = 1.230 GeV
K = 0.337 GeV
(b)
W = 1.500 GeV
K = 0.730 GeV
(c)
W = 2.51 GeV
K = 2.89 GeV
(d)
W = 4.2 GeV
K = 11.606GeV
$(d\sigma/d\Omega dE')/\Gamma_t$ $(10^{-30}\,cm^2)$
q^2 (GeV/c)^2
1416D1

Fig. 1

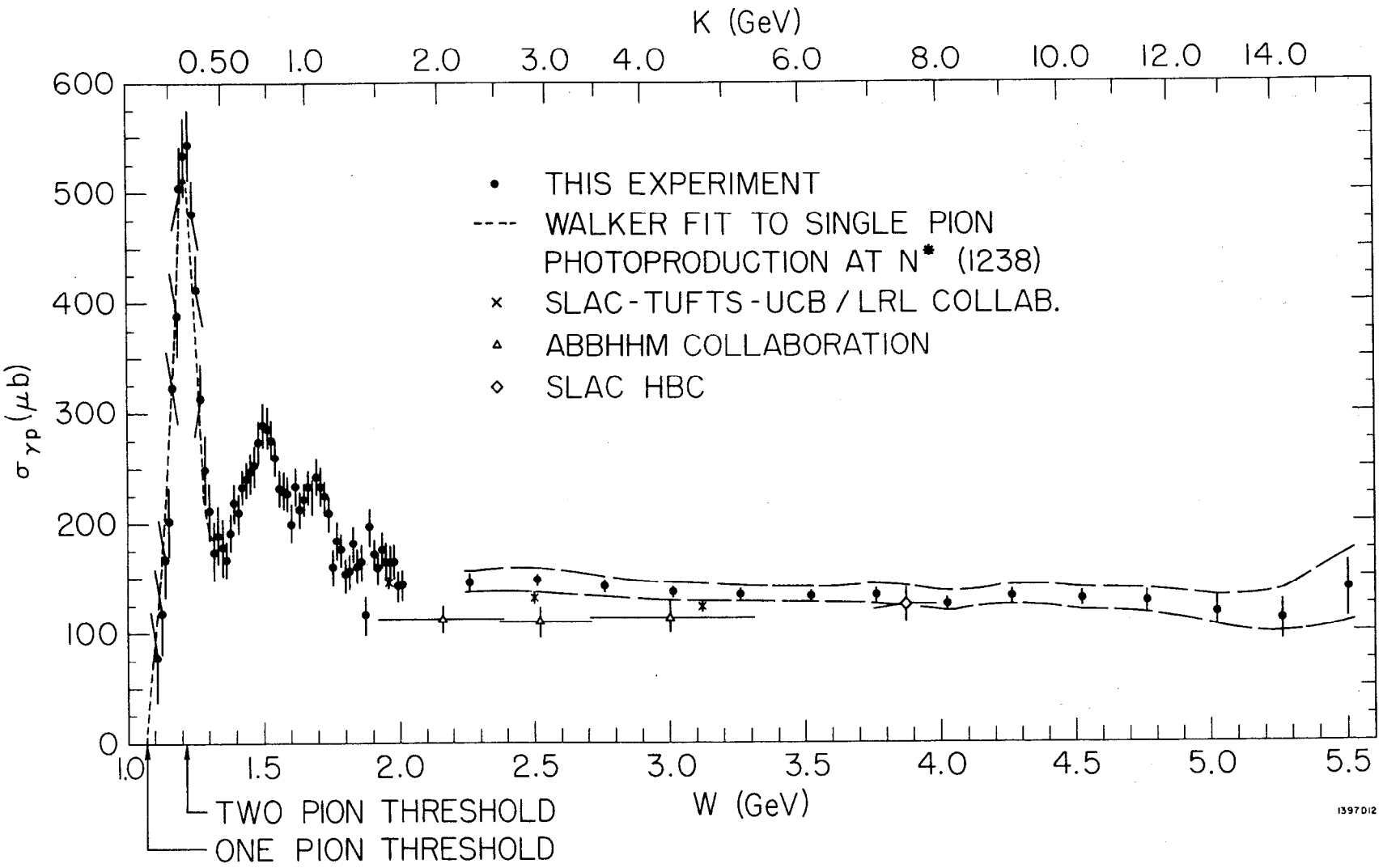
K (GeV)
0.50
1.0
2.0
3.0
4.0
6.0
8.0
10.0
12.0
14.0
600
500
400
300
200
100
0
$\sigma_{\gamma p}$ (μb)
THIS EXPERIMENT
WALKER FIT TO SINGLE PION PHOTOPRODUCTION AT N* (1238)
SLAC-TUFTS-UCB / LRL COLLAB.
ABBHHM COLLABORATION
SLAC HBC
1.0
1.5
2.0
2.5
3.0
3.5
4.0
4.5
5.0
5.5
W (GeV)
TWO PION THRESHOLD
ONE PION THRESHOLD
1397012

Fig. 2